Antiferromagnetic, metal-insulator, and superconducting phase transitions in underdoped cuprates: Slave-fermion t-J model in the hopping expansion

Akihiro Shimizu,[1] Koji Aoki,[1] Kazuhiko Sakakibara,[2] Ikuo Ichinose,[1] and Tetsuo Matsui[3,*]

[1]*Department of Applied Physics, Graduate School of Engineering, Nagoya Institute of Technology, Nagoya 466-8555, Japan*

[2]*Department of Physics, Nara National College of Technology, Yamatokohriyama 639-1080, Japan*

[3]*Department of Physics, Kinki University, Higashi-Osaka 577-8502, Japan*

(Received 23 July 2010; revised manuscript received 17 October 2010; published 9 February 2011)

We study a system of doped antiferromagnet in three dimensions at finite temperatures using the t-J model, a canonical model of strongly correlated electrons. We employ the slave-fermion representation of electrons, in which an electron is described as a composite of a charged spinless holon and a chargeless spinon. We introduce two kinds of U(1) gauge fields on links as auxiliary fields, one describing resonating valence bonds of antiferromagnetic nearest-neighbor spin pairs and the other for nearest-neighbor hopping amplitudes of holons and spinons in the ferromagnetic channel. To perform a numerical study of the system, we integrate out the fermionic holon field by using the hopping expansion in powers of the hopping amplitude, which is legitimate for the region in and near the insulating phase. The resultant effective model is described in terms of bosonic spinons, two U(1) gauge fields, and a collective field for hole pairs. We study this model by means of Monte Carlo simulations, calculating the specific heat, spin correlation functions, and instanton densities. We obtain a phase diagram in the hole concentration-temperature plane, which is in good agreement with that observed recently for clean and homogeneous underdoped samples.

DOI: 10.1103/PhysRevB.83.064502 PACS number(s): 74.72.−h, 11.15.Ha, 74.25.Dw

I. INTRODUCTION

Since the discovery of high-temperature superconductors of cuprates, more than two decades has passed.[1] Besides the high critical temperatures (T) of their superconducting (SC) phase transition, these cuprates have several interesting and anomalous properties.[2] To understand these properties, various theoretical approaches have been proposed.[3] Although ample knowledge have been accumulated, we still do not have a theory that has been accepted as the "right" one.

The t-J model[4] is one of the canonical models for high-T_c cuprates. In this model, doubly occupied electron states are excluded as a result of the strong on-site Coulomb repulsion between electrons. This constraint makes it hard to get a convincing understanding of the model such as its phase structure and properties of low-energy excitations. The slave-particle approach[5] using the slave-fermion or the slave-boson representation has been proposed to treat this local constraint on the physical states faithfully. In the slave-fermion representation, each electron is described as a composite of a charged spinless fermionic particle called a holon and a neutral bosonic particle with spin called a spinon. The mean-field theory based on the slave-particle representation is basically capable of describing various expected phases including the SC phase.[6] However, the result meets criticism that is common to every mean-field theory; that is, faithful evaluations of effects of fluctuations around mean fields are missing.

We have studied the t-J model in path-integral formalism by means of analytical methods aiming at going beyond the mean-field theory.[7] In the present paper, we revisit the t-J model on a three-dimensional (3D) cubic lattice in the slave-fermion path-integral representation, with the purpose of studying its properties nonperturbatively by means of *numerical methods*. To avoid the difficulty associated with fermionic determinants in numerical studies, we derive an effective model by employing the hopping expansion to evaluate integrals over fermionic holons. It is an expansion in powers of the hopping amplitude of holons. An effective expansion parameter is the hole concentration δ, and then the expansion is useful and legitimate at sufficiently low doping.

By studying the effective model by means of the Monte Carlo (MC) simulations, we obtain a phase diagram in the δ-T plane, which contains the antiferromagnetic (AF) phase, SC phase, and metal-insulator (MI) transition. The phase diagram obtained is in good agreement with that observed in experiments for lightly doped materials.[8]

The present paper is organized as follows. In Sec. II, we explain and set up the model in detail. The holon variables are analytically integrated out by means of the hopping expansion. The resultant model includes several bosonic variables: (i) the spinon field $z_{x\sigma}$, (ii) the auxiliary field for the spin-singlet amplitude of a nearest-neighbor spinon pair (we call it $U_{x\mu}$ in Sec. II), (iii) the auxiliary field for the amplitude of holon and spinon hoppings in the ferromagnetic (FM) channel ($V_{x\mu}$), which works as an order parameter of the MI transition, and (iv) the hole-pair field ($M_{x\mu}$) for superconductivity.

In Sec. III, we focus on the case without the superconducting channel (by neglecting the Ginzburg-Landau energy of the hole-pair field). We present the results of MC simulations for the corresponding model and locate the AF and MI phase transition lines.

In Sec. IV, we study the full model including the SC channel and discuss SC phase transitions together with AF and MI ones. We find that the SC state always occurs within the metallic phase, whereas AF long-range order (LRO) can coexist with the SC.

In Sec. V we present discussion and conclusions. We report that the present model offers us an interesting possibility for a new description of an SC state in the framework of gauge theory with *local interactions*.

In Appendix A, we present a discussion of the effect of bosonic thermal modes with nonvanishing Matsubara frequencies that are neglected for the bosonic spinon field in the text. In Appendix B we give some formulas for hopping expansion of the path integral over the fermionic holon field.

II. THE t-J MODEL IN THE SLAVE-FERMION REPRESENTATION AND HOLON HOPPING EXPANSION

A. Path integral expression

We start with the standard t-J model on a 3D cubic lattice,[9] whose Hamiltonian is given in terms of electron operator $C_{x\sigma}$ at site x $(=x_1,x_2,x_3)$ and spin σ $[=1(\uparrow),2(\downarrow)]$ as follows:

$$H = -t\sum_{x,\mu,\sigma}(\tilde{C}^\dagger_{x+\mu,\sigma}\tilde{C}_{x\sigma} + \text{H.c.}) + J\sum_{x,\mu}\left[\vec{S}_{x+\mu}\cdot\vec{S}_x - \frac{1}{4}n_x n_{x+\mu}\right], \tag{2.1}$$

where

$$\tilde{C}_{x\sigma} \equiv (1 - C^\dagger_{x\bar{\sigma}}C_{x\bar{\sigma}})\,C_{x\sigma}$$
$$\vec{S}_x \equiv \frac{1}{2}\sum_{\sigma,\sigma'}C^\dagger_{x\sigma}\vec{\sigma}_{\sigma\sigma'}C_{x\sigma'}\ \ (\vec{\sigma}:\text{Pauli matrices}), \tag{2.2}$$
$$n_x \equiv \sum_\sigma C^\dagger_{x\sigma}C_{x\sigma}$$

where $\mu(=1,2,3)$ is the 3D direction index and also denotes the unit vector. $\bar{\sigma}$ $(\bar{1}\equiv 2,\bar{2}\equiv 1)$ denotes the opposite spin. The doubly occupied states $(C^\dagger_{x\uparrow}C^\dagger_{x\downarrow}|0\rangle)$ are excluded from the physical states due to the strong on-site Coulomb repulsion. The operator $\tilde{C}_{x\sigma}$ respects this point.

We adopt the *slave-fermion representation* of the electron operator $C_{x\sigma}$ as a composite form,

$$C_{x\sigma} = \psi^\dagger_x a_{x\sigma}, \tag{2.3}$$

where ψ_x represents annihilation operator of the fermionic holon carrying the charge e and no spin, and $a_{x\sigma}$ represents annihilation operator of the bosonic spinon carrying $s = 1/2$ spin and no charge. Physical states $|\text{Phys}\rangle$ satisfy the following constraint:

$$\left(\sum_\sigma a^\dagger_{x\sigma}a_{x\sigma} + \psi^\dagger_x\psi_x\right)|\text{phys}\rangle = |\text{phys}\rangle. \tag{2.4}$$

In the salve-fermion representation, Hamiltonian (2.1) is given as

$$H = -t\sum_{x,\mu}(\psi^\dagger_x a^\dagger_{x+\mu}a_x\psi_{x+\mu} + \psi^\dagger_{x+\mu}a^\dagger_x a_{x+\mu}\psi_x) + \frac{J}{4}\sum_{x,\mu}[(a^\dagger\vec{\sigma}a)_{x+\mu}\cdot(a^\dagger\vec{\sigma}a)_x - (a^\dagger a)_{x+\mu}(a^\dagger a)_x],$$
$$(a^\dagger a)_x \equiv \sum_\sigma a^\dagger_{x\sigma}a_{x\sigma},\ (a^\dagger\vec{\sigma}a)_x \equiv \sum_{\sigma,\sigma'}a^\dagger_{x\sigma}\vec{\sigma}_{\sigma\sigma'}a_{x\sigma'}. \tag{2.5}$$

We employ the path-integral expression for the partition function of the t-J model,

$$Z = \text{Tr}\exp(-\beta H),\quad \beta \equiv \frac{1}{k_B T}, \tag{2.6}$$

at finite T in the slave-fermion representation. This is done by introducing a complex number $a_{x\sigma}(\tau)$ and a Grassmann number $\psi_x(\tau)$ at each site x and the imaginary time $\tau \in [0,\beta]$. Constraint (2.4) is solved[7] by introducing the CP^1 spinon variable $z_{x\sigma}(\tau)$, that is, two complex numbers z_{x1},z_{x2} for each site x satisfying

$$\sum_\sigma \bar{z}_{x\sigma}z_{x\sigma} = 1, \tag{2.7}$$

and writing

$$a_{x\sigma} = (1 - \bar{\psi}_x\psi_x)^{1/2}z_{x\sigma}. \tag{2.8}$$

It is easily verified that constraint (2.4) is satisfied by Eqs. (2.7) and (2.8). Then the partition function in the path-integral representation is given by an integral over the CP^1 variables $z_{x\sigma}(\tau)$ and Grassmann numbers $\psi_x(\tau)$.

We consider the system at finite and relatively high T's, such that *the τ dependence of the variables $z_{x\sigma}$ are negligible* (i.e., only their zero modes survive). Then the kinetic terms of $z_{x\sigma}$, $\bar{z}_x\partial z_x/\partial\tau$ disappear, and the T dependence may appear only as an overall factor β, which may be absorbed into the coefficients of the action. The τ dependence of the Grassmann variables $\psi_x(\tau)$ are taken into account in the τ-dependent holon propagator given in Appendix B. After integration over $\psi_x(\tau)$, the T dependence is absorbed into the holon densityδ. So one may still deal with the 3D model instead of the 4D model.

In general, study of finite-T properties of a system gives us an important insight into the low-T phase structure, for we can expect that ordered phases at finite T, which are found by the present method, should generally survive at $T = 0$. This expectation has been confirmed by previous studies of related models.[10,11] In Appendix A, we present some discussion of the physical meaning and reliability of the preceding approximation.

Then the partition function Z of the present 3D model at finite T's is given by the path integral[7]

$$Z = \int[dz][d\psi][dU]\exp A,\quad [dz] = \prod_x dz_x,$$
$$[d\psi] = \prod_x d\psi_x d\bar{\psi}_x,\quad [dU] = \prod_{x,\mu}dU_{x\mu}, \tag{2.9}$$

with the following action A on the 3D lattice:[13,14]

$$A = A_{\text{AF}} + A_{\text{hop}} + A_{\text{SC}},$$
$$A_{\text{AF}} = \frac{c_1}{2}\sum_{x,\mu}(z^\star_{x+\mu}U_{x\mu}z_x + \text{c.c.}),$$
$$A_{\text{hop}} = \frac{c_3}{2}\sum_{x,\mu}(\bar{z}_{x+\mu}z_x\bar{\psi}_x\psi_{x+\mu} + \text{c.c.}) - m\sum_x\rho_x, \tag{2.10}$$
$$A_{\text{SC}} = \frac{J\beta}{2}\sum_{x,\mu}\rho_{x+\mu}\rho_x|z^\star_{x+\mu}z_x|^2,$$

where

$$\begin{aligned} U_{x\mu} &\equiv \exp(i\theta_{x\mu}) \in U(1), \quad \rho_x \equiv \bar{\psi}_x \psi_x, \\ \bar{z}_{x+\mu} z_x &\equiv \bar{z}_{x+\mu,1} z_{x1} + \bar{z}_{x+\mu,2} z_{x2}, \\ z^\star_{x1} &\equiv z_{x2}, \quad z^\star_{x2} \equiv -z_{x1}, \\ z^\star_{x+\mu} z_x &= z_{x+\mu,2} z_{x1} - z_{x+\mu,1} z_{x2}. \end{aligned} \tag{2.11}$$

The first term $A_{\rm AF}$ in action A describes the AF coupling between nearest-neighbor (NN) spinons. We have introduced the U(1) gauge field $U_{x\mu}$ on the link $(x,x+\mu)$ as an auxiliary field to make the action in a simpler form and the U(1) gauge invariance (explained later) manifest. The second term $A_{\rm hop}$ describes simultaneous NN hopping of a holon and a spinon, keeping its spin orientation (i.e., in the FM channel). The third term, $A_{\rm SC}$, describes the attractive force between hole pairs, which we discuss in detail in Sec. II D. There are remaining terms,[15] which are irrelevant for discussion of the global phase structure.

The integration measures of $z_{x\sigma}$ and $U_{x\mu}$ are

$$\begin{aligned} \int dz_x &= \prod_\sigma \int_{-\infty}^{\infty} d\,{\rm Re} z_{x\sigma} \int_{-\infty}^{\infty} d\,{\rm Im} z_{x\sigma} \cdot \delta\left(\sum_\sigma \bar{z}_{x\sigma} z_{x\sigma} - 1\right), \\ \int dU_{x\mu} &= \int_{-\pi}^{\pi} \frac{d\theta_{x\mu}}{2\pi}. \end{aligned} \tag{2.12}$$

Grassmann variables ψ_x anticommute each other:

$$[\psi_x, \psi_{x'}]_+ = [\psi_x, \bar{\psi}_{x'}]_+ = [\bar{\psi}_x, \bar{\psi}_{x'}]_+ = 0. \tag{2.13}$$

The formulas of Grassmann integration[16] are

$$\int d\psi_x d\bar{\psi}_x [1, \psi_x, \bar{\psi}_x, \bar{\psi}_x \psi_x] = [0,0,0,1]. \tag{2.14}$$

The term $m \sum_x \bar{\psi}_x \psi_x$ adjusts the hole density to δ as

$$\langle \bar{\psi}_x \psi_x \rangle = \delta. \tag{2.15}$$

Therefore the parameter m works as (the negative of) the chemical potential.

The action A is invariant under a local (x-dependent) U(1) gauge transformation with a gauge function λ_x[17]

$$z_{x\sigma} \to e^{i\lambda_x} z_{x\sigma}, \quad U_{x\mu} \to e^{-i\lambda_{x+\mu}} U_{x\mu} e^{-i\lambda_x}, \quad \psi_x \to e^{i\lambda_x} \psi_x. \tag{2.16}$$

B. AF and ferromagnetic spinon amplitudes

The gauge field $U_{x\mu}$ is related to the spinon field z_x as

$$\langle U_{x\mu} \rangle \sim \overline{\left\langle \frac{z^\star_{x+\mu} z_x}{|z^\star_{x+\mu} z_x|} \right\rangle}, \tag{2.17}$$

which is obtained by maximizing the action $A_{\rm AF}$. Therefore $U_{x\mu}$ describes the (c.c. of) phase factor of the AF NN spin-pair amplitude $z^\star_{x+\mu} z_x$ in Eq. (2.11). In fact, one can integrate out $U_{x\mu}$ in Eq. (2.9) and obtain

$$\begin{aligned} \int [dU] \exp(A_{\rm AF}) &= \exp(\tilde{A}_{\rm CP^1}), \\ \tilde{A}_{\rm CP^1} &= \sum_{x\mu} \log I_0(c_1 |z^\star_{x+\mu} z_x|), \end{aligned} \tag{2.18}$$

where I_0 is the modified Bessel function. The effective term $\tilde{A}_{\rm CP^1}$ should be compared with the original expression $A_{\rm CP^1}$ of the CP^1 model:

$$Z_{\rm CP^1} = \int [dz] \exp(A_{\rm CP^1}), \quad A_{\rm CP^1} = \frac{\beta J}{2} \sum_{x,\mu} |z^\star_{x+\mu} z_x|^2. \tag{2.19}$$

This CP^1 model describes the t-J model without holes ($c_3 = 0$, $A_{\rm SC} = 0$), that is, the AF Heisenberg spin model at finite T. Note that the amplitude $z^\star_{x+\mu} z_x$ between NN spinon pair reads explicitly as

$$z^\star_{x+\mu} z_x = z_{x+\mu,2} z_{x1} - z_{x+\mu,1} z_{x2}. \tag{2.20}$$

This expresses the amplitude of spin-singlet AF combination of NN spinons, which is called the RVB. Both models with $A_{\rm CP^1}$ and $\tilde{A}_{\rm CP^1}$ have similar behavior and it is verified that they give rise to second-order transitions at certain c_1 and J.[18] The parameters c_1 in the action (2.10) are related to the original ones as[18]

$$c_1 \sim \begin{cases} J\beta & \text{for } c_1 \gg 1, \\ (2J\beta)^{1/2} & \text{for } c_1 \ll 1. \end{cases} \tag{2.21}$$

For the coupling c_3, the relation is straightforward:

$$c_3 \sim t\beta. \tag{2.22}$$

Let us explore the meaning of the CP^1 term $A_{\rm AF}$ (the AF spin coupling) and the hopping term $A_{\rm hop}$ (the t term) further. For this purpose, it is convenient to introduce an O(3) spin vector field $\vec{\ell}_x$ made of spinon z_x:

$$\vec{\ell}_x \equiv \bar{z}_x \vec{\sigma} z_x = \sum_{\sigma,\sigma'} \bar{z}_{x\sigma} \vec{\sigma}_{\sigma\sigma'} z_{x\sigma'}, \quad \vec{\ell}_x \cdot \vec{\ell}_x = 1. \tag{2.23}$$

The NN spin correlation $\vec{\ell}_{x+\mu} \cdot \vec{\ell}_x$ is expressed by the CP^1 amplitudes (such as $\bar{z}_{x+\mu} z_x$) as

$$\begin{aligned} \vec{\ell}_{x+\mu} \cdot \vec{\ell}_x &= 2|\bar{z}_{x+\mu} z_x|^2 - 1 \\ &= -2|z^\star_{x+\mu} z_x|^2 + 1, \end{aligned} \tag{2.24}$$

where we have used the identity,

$$|\bar{z}_{x+\mu} z_x|^2 + |z^\star_{x+\mu} z_x|^2 = 1. \tag{2.25}$$

So if the spinon hopping amplitude $\bar{z}_{x+\mu} z_x$ that appears in $A_{\rm hop}$ has an absolute value near its maximum, $|\bar{z}_{x+\mu} z_x| \sim 1$, then the NN spins are mostly FM $\vec{\ell}_{x+\mu} \cdot \vec{\ell}_x \sim 1$. In contrast, if the spinon RVB amplitude $z^\star_{x+\mu} z_x$ takes values with $|z^\star_{x+\mu} z_x| \sim 1$, then the NN spins are mostly AF, $\vec{\ell}_{x+\mu} \cdot \vec{\ell}_x \sim -1$. These two amplitudes satisfy the sum rule, Eq. (2.25). The AF phase and FM phase are characterized by LRO in the spin correlation function $\langle \vec{\ell}_x \cdot \vec{\ell}_y \rangle$, and they can coexist with each other as we see in the following sections.

C. Holon hopping expansion and auxiliary field $V_{x\mu}$

In Eq. (2.9), one can integrate out the fermionic holon field ψ_x by assuming a low holon density δ of Eq. (2.15). In this region, the hopping expansion of ψ_x is applicable as it is an

expansion in powers of δ. Some details of the integration of ψ_x are given in Appendix B. After integration over ψ_x we obtain

$$\int [d\psi] \exp(A_{\rm hop}) = \exp(\tilde{A}_{\rm hop}),$$
$$\tilde{A}_{\rm hop} = \delta\left(\frac{c_3}{2}\right)^2 \sum_{x,\mu} |\bar{z}_{x+\mu} z_x|^2 + \delta\left(\frac{c_3}{2}\right)^4 \sum_{x,\mu<\nu} \prod_{\rm plaq.} (\bar{z}_{x+\mu} z_x) + \cdots. \tag{2.26}$$

The second term of $\tilde{A}_{\rm hop}$ denotes the product of $\bar{z}_{x+\mu} z_x$ on the link $(x, x+\mu)$ [$\bar{z}_x z_{x+\mu}$ on the link $(x+\mu, x)$] around the plaquette $(x, x+\mu, x+\mu+\nu, x+\nu)$, and the ellipsis denotes nonlocal higher-order terms. Both the first and the second terms favor FM couplings of NN spin pairs.

Then we introduce a vector field $W_{x\mu}$ as an auxiliary field corresponding to $\bar{z}_x z_{x+\mu}$,

$$\langle W_{x\mu} \rangle \sim \langle \bar{z}_x z_{x+\mu} \rangle, \tag{2.27}$$

by using Gaussian integration (Hubbard-Stratonovich transformation) as follows:

$$\exp(\tilde{A}_{\rm hop}) = \int [dW] \exp(A_W),$$
$$A_W = \delta\left(\frac{c_3}{2}\right)^2 \left(-\sum_{\rm x,\mu} |W_{x\mu}|^2 + \sum_{x,\mu} (\bar{z}_{x+\mu} z_x W_{x\mu} + \text{c.c.}) \right) + \delta\left(\frac{c_3}{2}\right)^4 \sum_{x,\mu<\nu} \prod_{\rm plaq.} W_{x\mu} + \cdots. \tag{2.28}$$

Estimation of the magnitude of $W_{x\mu}$ is straightforward for $T/J \leqslant 1$ as

$$\int [dz] e^{-\frac{J}{2}\beta |\bar{z}_{x+\mu} z_x|^2} |\bar{z}_{x+\mu} z_x|^2 \sim \frac{1}{J\beta}. \tag{2.29}$$

Then we set

$$W_{x\mu} = W V_{x\mu}, \quad W \simeq \frac{1}{\sqrt{J\beta}}, \quad V_{x\mu} = \exp(i\varphi_{x\mu}) \in \mathrm{U}(1), \tag{2.30}$$

by ignoring the fluctuation of the radial component of $W_{x\mu}$ and focusing on its phase, $dW_{x\mu} \to dV_{x\mu} \equiv d\varphi_{x\mu}/(2\pi)$. So the correspondence, Eq. (2.27), becomes

$$\langle V_{x\mu} \rangle \sim \left\langle \frac{\bar{z}_x z_{x+\mu}}{|\bar{z}_x z_{x+\mu}|} \right\rangle. \tag{2.31}$$

This simplification is based on the observation that the most relevant degrees of freedom in gauge theories are the phases of gauge fields on the links rather than the amplitude W because the latter has only massive excitations. The phase factor $V_{x\mu}$ is a new U(1) gauge field that transforms under gauge transformation (2.16) as

$$V_{x\mu} \to e^{i\lambda_{x+\mu}} V_{x\mu} e^{-i\lambda_x}. \tag{2.32}$$

The physical meaning of $V_{x\mu}$ is obvious from the discussion given in Sec. II B. It measures the phase part of the SR FM spinon channel, the deviation from the AF order. Its coherent "condensation" induces coherent hopping of holons ψ_x in the FM spinon channel, as the term $A_{\rm hop}$ shows, and therefore an MI transition into a metallic phase. More detailed discussion is given in the following sections.

The $A_{\rm hop}$ term is then rewritten effectively as follows:

$$\exp(\tilde{A}_{\rm hop}) = \int [dV] \exp(A_V),$$
$$A_V = \frac{c_4}{2} \sum_{x,\mu} (V_{x\mu} \bar{z}_{x+\mu} z_x + \text{c.c.}) + \frac{c_5}{2} \sum_{x,\mu<\nu} (\bar{V}_{x\nu} \bar{V}_{x+\nu,\mu} V_{x+\mu,\nu} V_{x\mu} + \text{c.c.}),$$
$$\int [dV] = \prod_{x,\mu} \int_{-\pi}^{\pi} \frac{d\varphi_{x\mu}}{2\pi}. \tag{2.33}$$

We have neglected the higher-order terms in Eq. (2.26), as they have smaller coefficients for $T/J < 1$ with numerical damping factors. However, effects of these nonlocal terms can be expected qualitatively. As they have all positive coefficients, all of them favor the order of the field $V_{x\mu}$ and, so, the metallic phase. From this point of view, the critical hole concentration δ_c of the MI transition obtained by the numerical study in Sec. IV might give an overestimation of the true value.

The parameters c_4 and c_5 in A_V are related to the original ones as

$$c_4 \sim \frac{\delta c_3^2}{J\beta} \sim \frac{\delta t^2 \beta}{J}, \quad c_5 \sim \frac{\delta c_3^4}{(J\beta)^2} \sim \frac{\delta t^4 \beta^2}{J^2}. \tag{2.34}$$

In the following investigation of the phase diagram of the system, however, we treat c_4 and c_5 in a more flexible manner, as free parameters that are proportional to δ and are increasing functions of $\beta = 1/T$. As most phase transitions in the present model appear in the region $c_1 \gg 1$, we identify T and δ from Eqs. (2.21) and (2.34) as

$$T \simeq \frac{J}{c_1}, \quad \delta \simeq \frac{J^2}{t^2} \frac{c_4}{c_1}. \tag{2.35}$$

At this stage, the original partition function Z without $A_{\rm SC}$ is expressed as

$$Z \to Z_{UV} \equiv \int [dz][dU][dV] \exp(A_{UV}),$$
$$A_{UV} = A_{\rm AF}(z_x, U_{x\mu}) + A_V(z_x, V_{x\mu}). \tag{2.36}$$

This "UV" model describes the competition between the AF-RVB spin-pair amplitude $U_{x\mu}$ and the FM spin-hopping amplitude $V_{x\mu}$; the latter is generated by integration over holon hopping.

D. Hole-pair field $M_{x\mu}$ and the full model $A_{\rm full}$

As shown in the previous section, in the effective action, Eq. (2.10), there exists the term $A_{\rm SC}$, which describes an attractive force between NN holes doped in AF magnets or, more precisely, in an SR AF background. This attractive force comes from the J terms in Hamiltonian (2.5). Actually, two holes with a mutual distance of more than one lattice spacing break 12 AF bonds of spins, while a pair of holes at NN sites breaks just 11 AF bonds. Thus the NN hole pair is favored

energetically. To see it explicitly, we rewrite $A_{\rm SC}$ in Eq. (2.10) as follows:

$$A_{\rm SC} = \frac{J\beta}{2}\sum_{x,\mu}|\bar{\psi}_{x+\mu}(z^{\star}_{x+\mu}z_x)\bar{\psi}_x|^2. \tag{2.37}$$

Note that the holon-pair variable $\bar{\psi}_{x+\mu}\bar{\psi}_x$ is accompanied by the RVB spinon-pair amplitude $z^{\star}_{x+\mu}z_x$. This combination is nothing but $C_{x+\mu,2}C_{x1} - C_{x+\mu,1}C_{x2}$ in terms of electron operators. We expect that this attractive force induces hole-pair condensation under certain conditions, and as a result, a SC state is generated. The main problem addressed here is whether this attractive force is strong enough to generate a SC state in the region *without* AF LRO.

To investigate a possible SC phase transition, we introduce a hole-pair field $M_{x\mu}$ as a complex auxiliary field describing the configuration of a holon pair accompanied by an RVB spinon pair at sites x and $x+\mu$. So $M_{x\mu}$ should satisfy

$$\langle M_{x\mu}\rangle \sim \langle\bar{\psi}_{x+\mu}(z^{\star}_{x+\mu}z_x)\bar{\psi}_x\rangle. \tag{2.38}$$

This hole-pair field $M_{x\mu}$ is nothing but the annihilation operator of spin-singlet electron-pair sitting NN sites as mentioned. Explicitly, we use the Hubbard-Stratonovich transformation for $A_{\rm SC}$ as in Eq. (2.28):

$$\begin{aligned}\exp&\left(\frac{J}{4}|\bar{\psi}_{x+\mu}(z^{\star}_{x+\mu}z_x)\bar{\psi}_x|^2\right)\\ &= \int dM_{x\mu}\exp\left[-\frac{J\beta}{4}\bar{M}_{x\mu}M_{x\mu}\right.\\ &\quad\left.+\frac{J\beta}{4}(M_{x\mu}\psi_x(\bar{z}^{\star}_{x+\mu}\bar{z}_x)\psi_{x+\mu}+\text{c.c.})\right].\end{aligned} \tag{2.39}$$

This assures us of Eq. (2.38).

To study the effect of $A_{\rm SC}$, we start with Z of Eq. (2.10) and rewrite $A_{\rm SC}$ in the action by using Eq. (2.39). Then we integrate out the holon variables ψ_x as in the previous case (without $A_{\rm SC}$ there) to obtain the effective action $A_{\rm full}$, where the subscript "full" implies that $A_{\rm SC}$ is taken into account. The partition function of the full model is now given as

$$\begin{aligned}Z_{\rm full} &\equiv \int[dz][dU][dV][dM]\exp(A_{\rm full}),\\ A_{\rm full} &= A_{UV}+A_M = A_{\rm AF}+A_V+A_M.\end{aligned} \tag{2.40}$$

In addition to the action of the UV model of Eq. (2.36), $A_{\rm full}$ includes an extra term $A_{\rm M}(z_x, M_{x\mu})$ which depends on z_x and $M_{x\mu}$.

We have calculated A_M in the order up to $O[(c_3)^4]$.[7] Equation (2.39) shows that as ψ_x and $\psi_{x+\mu}$ hop, they leave the factor $M_{x\mu}\bar{z}^{\star}_{x+\mu}\bar{z}_x$, that is, $M_{x\mu}$ is always accompanied by the AF component of the spinon (c.c. of) $z^{\star}_{x+\mu}z_x$. The hopping term $A_{\rm hop}$ itself supplies the FM component $\bar{z}_xz_{x+\nu}(\sim|\bar{z}_xz_{x+\nu}|V_{x\nu})$ along the link $(x,x+\nu)$ ψ_x hops. In expressing A_M we prefer to use $U_{x\mu}$ instead of $\bar{z}^{\star}_{x+\mu}\bar{z}_x$ using Eq. (2.17), because it makes the gauge invariance of the system manifest. Then $M_{x\mu}$ appears in A_M in the combination $M_{x\mu}(\bar{z}^{\star}_{x+\mu}\bar{z}_x)\sim M_{x\mu}|z^{\star}_{x+\mu}z_x|U_{x\mu}$. So we define a new variable,

$$M^{\star}_{x\mu}\equiv M_{x\mu}U_{x\mu}\sim\bar{\psi}_{x+\mu}\bar{\psi}_x, \tag{2.41}$$

and write A_M in terms of $M^{\star}_{x\mu}$ and $V_{x\mu}$; the latter is supplied by $A_{\rm hop}$. We note that $M^{\star}_{x\mu}$ is not gauge invariant and represents the "holon pair" at $(x,x+\mu)$, in contrast with the gauge-invariant $M_{x\mu}$ for the "hole pair."

In the practical calculations in Sec. IV, we focus on the phase degrees of freedom of $M^{\star}_{x\mu}$, ignoring fluctuations of the radial part of $M^{\star}_{x\mu}$ as in the case of $W_{x\mu}\to V_{x\mu}$ (the London limit). So we set

$$M^{\star}_{x\mu} = M\exp(i\varphi_{x\mu}),\quad M\simeq\sqrt{\text{holon-pair density}}\sim\delta, \tag{2.42}$$

and $dM_{x\mu} = d\varphi_{x\mu}/(2\pi)$. We include M into the coefficients of $A_{\rm M}$ and treat $M_{x\mu}=\exp(i\varphi_{x\mu})$ as a U(1) variable. Furthermore, we regard $|\bar{z}_xz_{x+\mu}|$ and $|z^{\star}_{x+\mu}z_x|$ involved in A_M as constants. They are also absorbed in the coefficients. The reason for this treatment is given here in the determination of the coefficients.

In terms of this $M^{\star}_{x\mu}$, A_M is expressed as

$$\begin{aligned}A_M = &\frac{f_1}{2}\sum_{x,\mu\neq\nu}M^{\star}_{x\mu}\bar{M}^{\star}_{x+\nu,\mu}V_{x+\mu,\nu}V_{x\nu}+\frac{f_2}{2}\sum_{x,\mu<\nu}\alpha_{\mu\nu}\\ &\times[V_{x\nu}V_{x+\nu,\mu}\bar{M}^{\star}_{x+\mu,\nu}M^{\star}_{x\mu}+V_{x\nu}\bar{M}^{\star}_{x+\nu,\mu}M^{\star}_{x+\mu,\nu}\bar{V}_{x\mu}\\ &+M^{\star}_{x\nu}\bar{M}^{\star}_{x+\nu,\mu}V_{x+\mu,\nu}V_{x\mu}+\bar{M}^{\star}_{x\mu}\bar{V}_{x+\nu,\mu}V_{x+\mu,\nu}M^{\star}_{x\mu}]\\ &+\frac{f_3}{2}\sum_{x,\mu<\nu}\bar{M}^{\star}_{x\nu}M^{\star}_{x+\nu,\mu}\bar{M}^{\star}_{x+\mu,\nu}M^{\star}_{x\mu}+\text{c.c.}\end{aligned} \tag{2.43}$$

Each term in A_M is shown schematically in Fig. 1. The terms with the coefficients f_1 and f_2 in Eq. (2.43) describe the local hopping of the holon-pair field $M^{\star}_{x\mu}$, whereas the f_3 term controls fluxes of $M^{\star}_{x\mu}$ penetrating each plaquette. These fluxes correspond to vortex excitations in the SC state. In other words, the f_1 and f_2 terms induce a primordial SC state, and a genuine SC state is generated by the f_3 term. Numerical investigations in the following sections verify this qualitative expectation.

As stated in Sec. I, we think that an SC state is to be realized in a metallic phase, that is, beyond the region of applicability of the leading order of the hopping expansion. So keeping the results of the hopping expansion for the three coefficients f_i of A_M is not suitable for discussion of an SC state. For example, the coefficient f_3 is negative in the leading order of the hopping expansion, which favors the $s+id$–wave SC. We examined higher-order terms of the hopping expansion and found that some of them generate a positive value of f_3 to support the d-wave SC as observed experimentally. So in the following numerical studies, we assume that f_i's are positive and proportional to δ^2,

$$f_1, f_2, f_3\propto\delta^2, \tag{2.44}$$

and treat their coefficients as *positive* free (phenomenological) parameters.[19] In short, all effects of $|M_{x\mu}|$, $|\bar{z}_xz_{x+\mu}|$ and $|z^{\star}_{x+\mu}z_x|$ in and near the SC state are included in the effective coefficients f_i of A_M.

Also, we have incorporated in Eq. (2.43) the layered structure of the 3D lattice of cuprates[9] by introducing in Eq. (2.43) the anisotropy parameter $\alpha_{\mu\nu}$, which is defined as

$$\alpha_{\mu\nu}=\alpha_{\nu\mu}=\begin{cases}1 & (\mu,\nu\neq 3).\\ 0 & (\mu\text{ or }\nu=3).\end{cases} \tag{2.45}$$

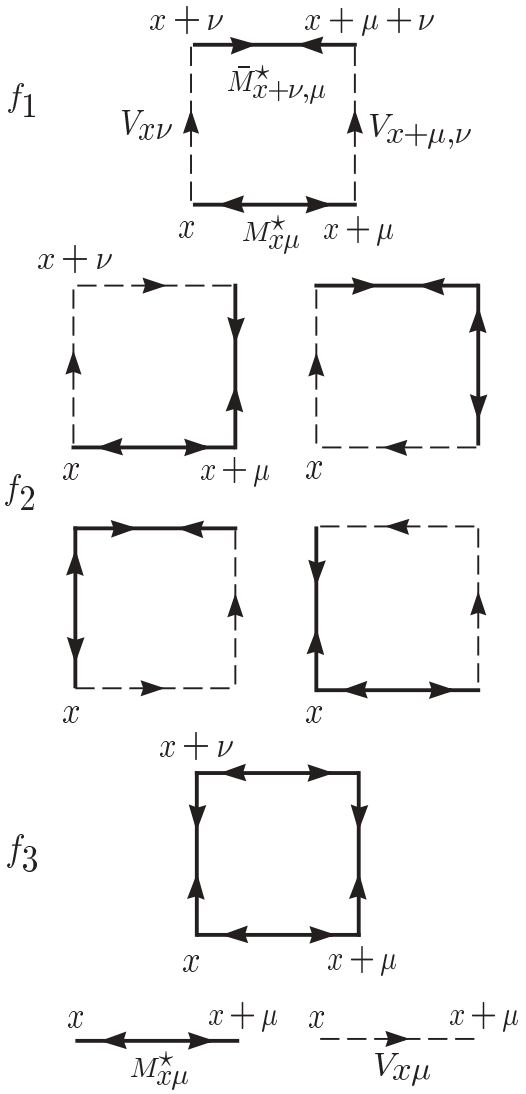

FIG. 1. Each term of $A_{\rm M}$ in Eq. (2.43). Lines with reversed arrows indicate complex-conjugate variables, $\bar{M}^{\star}_{x\mu}$ and $\bar{V}_{x\mu}$. The gauge invariance under Eq. (2.16) forces the arrows near each corner to make a divergenceless flow.

The layered structure of the system is systematically incorporated in the original Hamiltonian (2.1) by making the parameters t and J anisotropic. This induces anisotropies in the effective model that we have derived. Most of the terms are insensitive to the anisotropy, except the f_2 term, which is the reason that we treat $A_{\rm hop}$ and A_V in a symmetric manner. For the f_2 term, the layered structure plays an important role to avoid frustrations and make the symmetry of SC be $d_{x^2-y^2}$.

III. PHASE STRUCTURE OF THE UV MODEL: AF AND MI TRANSITIONS

In this section, we study the UV model with the action $A_{UV} = A_{\rm AF} + A_V$ in Eq. (2.36) by means of MC simulations. The full model $A_{\rm full} = A_{\rm AF} + A_V + A_M$ is studied in Sec. IV. For MC simulations, we consider a 3D cubic lattice of the size $V \equiv L^3$ (L up to 30) with the periodic boundary condition. We used the standard Metropolis algorithm with the local update. The average number of sweeps was 2×10^5, and the acceptance ratio was about $\sim$40%.

To study the phase structure of the model, we measured the internal energy E and the specific heat C, which are defined as

$$E = -\frac{1}{L^3}\langle A\rangle, \quad C = \frac{1}{L^3}\langle (A - \langle A\rangle)^2\rangle, \tag{3.1}$$

as functions of the parameters c_1, c_4, and c_5. We note that the c_4 term and c_5 term are related to each other because both are generated by the c_3 term. Here we respect this correlation by setting the parameter c_5 as $c_5 \propto c_4$.

By obtaining the locations of the phase transition lines by the peaks of C, etc., we get a phase diagram in the c_4-c_1 plane. Then we investigate spin correlation functions and instanton densities to identify the physical meaning and properties of each phase. To support this procedure, we also investigated fluctuations of each term of the action by measuring the individual "specific heat" C_{Ai} defined by

$$\begin{aligned} C_{A_i} &\equiv \frac{1}{L^3}\langle (A_i - \langle A_i\rangle)^2\rangle, \quad i = 1,4,5, \\ A_1 &\equiv A_{\rm AF}, \quad A_{4,5} \equiv c_{4,5} \text{ term in } A_V. \end{aligned} \tag{3.2}$$

At $c_4 = 0$ (i.e., at $c_3 = 0$), the system is reduced to the AF Heisenberg model with the action $A_{\rm AF}$ alone, which has a phase transition from the paramagnetic (PM) spin-disordered phase to the AF spin-ordered phase at $c_1 \sim 2.8$. We study how the location of this AF phase transition changes and whether new phases appear as the c_4 term is turned on. It is naturally expected that the AF phase transition shifts to the low-T region (large c_1 region), as the parameter c_4 is increased because the c_4 term favors FM NN spin coupling.

Let us first examine C and C_{A_i} as functions of c_4 for $c_1 = 3.5$. As we shall see, this value of c_1 belongs to a relatively high-T region. In Fig. 2 we show the result for the case $c_5 = c_4/3.0$. We found no anomalous behavior of E such as hysteresis, whereas C shown in Fig. 2 exhibits two sharp peaks at $c_4 \simeq 1.5$ and 3.0. We verified that each peak has a systematic system-size (L) dependence, so we concluded that both peaks show existence of second-order phase transitions. C_{A_1} in Fig. 2 exhibits a very sharp peak at $c_4 \simeq 1.5$. In contrast, both C_{A_4} and C_{A_5} exhibit a peak at $c_4 \simeq 3.0$. Then we conclude that the AF phase transition takes place at $c_4 \simeq 1.5$ and the MI transition at $c_4 \simeq 3.0$.

This conclusion may be confirmed by calculating the spin correlation function. In Fig. 3, we show the correlation function $G_{\rm s}(r)$ of the O(3) spin $\vec{\ell}_x$ of Eq. (2.23):

$$G_{\rm s}(r) = \frac{1}{3L^3}\sum_{x,\mu}\langle \vec{\ell}_x \cdot \vec{\ell}_{x+r\mu}\rangle. \tag{3.3}$$

As we expected, at $c_4 = 0.7$, $G_{\rm s}(r)$ exhibits an oscillatory behavior and has a staggered magnetization:

$$\begin{aligned} \lim_{r\to\infty}(-)^r G_{\rm s}(r) &\simeq (-)^{r_{\rm max}} G_{\rm s}(r_{\rm max}) \neq 0, \\ r_{\rm max} &\equiv \frac{L}{2} \quad \text{(AF phase)}. \end{aligned} \tag{3.4}$$

So there exists an AF LRO at $c_4 = 0.7$. This confirms that the phase transition at $c_4 \simeq 1.5$ is the AF transition. At $c_4 = 2.2$

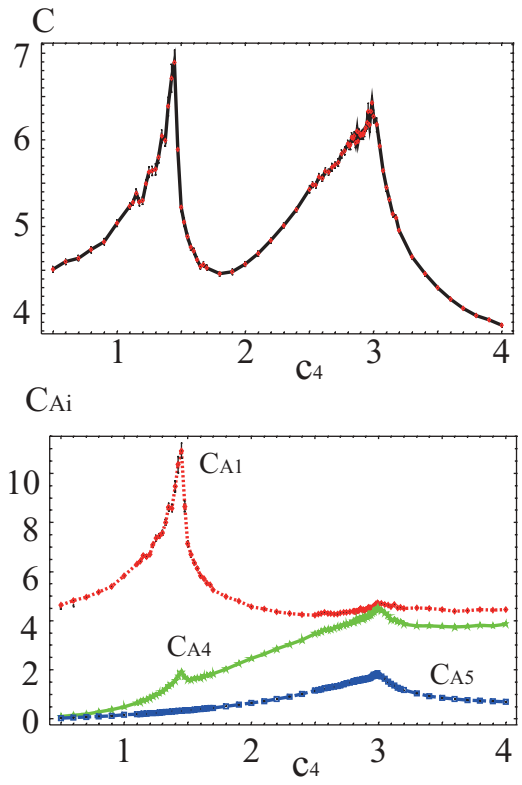

FIG. 2. (Color online) Total specific heat C and specific heat of each term C_{A_i} of Eq. (3.2) as functions of c_4 for $c_1 = 3.5$ and $c_5 = c_4/3.0$. System size is $L = 30$. C has two peaks, at $c_4 \simeq 1.5, 3.0$. C_{A_1} has a sharp peak at $c_4 \simeq 1.5$, suggesting an AF transition, and C_{A_4}, C_{A_5} have peaks at $c_4 \simeq 3.0$, suggesting an MI transition.

this AF order disappears and the system is in a magnetically disordered phase that we call the PM phase. At $c_4 = 3.8$, $G_s(r)$ exhibits LRO,

$$G_s(r_{\max}) \neq 0 \quad \text{(FM phase)}, \tag{3.5}$$

which implies that the system is in the FM phase. So we obtain a picture of the phase structure for $c_1 = 3.5$ wherein, as c_4 increases, the phase changes as AF $\rightarrow$ PM $\rightarrow$ FM.

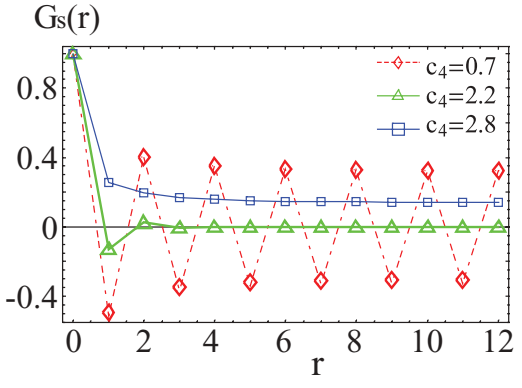

FIG. 3. (Color online) Spin correlation function $G_s(r)$ of Eq. (3.3) for $c_1 = 3.5$, $c_5 = c_4/3.0$, and $L = 24$. At $c_4 = 0.7$, AF LRO exists. At $c_4 = 2.2$, the AF LRO disappears. At $c_4 = 3.8$, an FM correlation appears as a result of the existence of "free electrons."

We also calculated instanton densities of the gauge fields $U_{x\mu}$ and $V_{x\mu}$. For example, the U-instanton density ρ_U is defined for $U_{x\mu} = e^{i\theta_{x\mu}}$, $\theta_{x\mu} \in [-\pi, \pi]$ in the following way.[18,20] We first consider the magnetic flux $\Theta_{x\mu\nu}$ penetrating the plaquette $(x, x+\mu, x+\mu+\nu, x+\nu)$, which is defined as

$$\Theta_{x\mu\nu} \equiv \theta_{x\mu} + \theta_{x+\mu,\nu} - \theta_{x+\nu,\mu} - \theta_{x\nu} (-4\pi \leqslant \Theta_{x\mu\nu} \leqslant 4\pi). \tag{3.6}$$

Then we decompose $\Theta_{x\mu\nu}$ into its integer part $n_{x\mu\nu}$, which represents the Dirac string (vortex line), and the remaining fractional part $\tilde{\Theta}_{x\mu\nu}$,

$$\Theta_{x\mu\nu} = 2\pi n_{x\mu\nu} + \tilde{\Theta}_{x\mu\nu} \quad (-\pi \leqslant \tilde{\Theta}_{x\mu\nu} \leqslant \pi). \tag{3.7}$$

The U-instanton density $\rho_U(x)$ at the cube around site $x + \frac{\hat{1}}{2} + \frac{\hat{2}}{2} + \frac{\hat{3}}{2}$ of the dual lattice is then defined as

$$\begin{aligned} \rho_U(x) &= -\frac{1}{2} \sum_{\mu\nu\lambda} \epsilon_{\mu\nu\lambda} (n_{x+\mu,\nu\lambda} - n_{x,\nu\lambda}) \\ &= \frac{1}{4\pi} \sum_{\mu,\nu,\lambda} \epsilon_{\mu\nu\lambda} (\tilde{\Theta}_{x+\mu,\nu\lambda} - \tilde{\Theta}_{x,\nu\lambda}), \end{aligned} \tag{3.8}$$

where $\epsilon_{\mu\nu\lambda}$ is the totally antisymmetric tensor. From this definition, we define the average instanton density ρ_U as

$$\rho_U \equiv \frac{1}{L^3} \sum_x \langle |\rho_U(x)| \rangle. \tag{3.9}$$

The V-instanton density ρ_V is defined similarly for $V_{x\mu}$.

The instanton density ρ_U measures strength of fluctuations of the gauge field $U_{x\mu}$. In the deconfinement phase of $U_{x\mu}$, fluctuations of $\Theta_{x\mu\nu}$ around its average $\Theta_{x\mu\nu} = 0$ are small and $\rho_U \simeq 0$. In the confinement phase of $U_{x\mu}$, in contrast, $\Theta_{x\mu\nu}$ fluctuates violently, and ρ_U has a finite value. Here we note that the confinement by the $U_{x\mu}$ field gives rise to quasiexcitations that are gauge-invariant "composite particles" in the AF channel. Such combinations include $z^\star_{x+\mu} U_{x\mu} z_x$, $\psi_{x+\mu} U_{x\mu} z_{x\sigma}$, etc. A similar interpretation holds for ρ_V concerning the gauge dynamics of $V_{x\mu}$. The confinement here works in the FM channel, and the possible gauge-invariant quasiexcitations are $\bar{\psi}_x z_{x\sigma} = C_{x\sigma}$, $\bar{\psi}_x \psi_x$, $\bar{z}_{x\sigma} z_{x\sigma'}$, and their stretched versions such as $\bar{\psi}_{x+\mu} V_{x\mu} z_{x\sigma}$.

In Fig. 4 we show ρ_U and ρ_V for $c_1 = 3.5$. As we increase c_4, ρ_U starts to increase at the first phase transition at $c_4 \simeq 1.5$. This result means that the fluctuation of $U_{x\mu}$ of AF NN spinon pairs become large, and the U-confinement spin-disordered phase appears. This result is consistent with the previous interpretation based on $G_s(r)$ above. In contrast, at the second phase transition at $c_4 \simeq 3.0$, ρ_V tends to vanish. So, for $c_4 < 3.0$, the system stays in the V-confinement phase, and holons and antispinons are bound within electrons as $\psi_x \bar{z}_{x\sigma}$. For $c_4 > 3.0$, the system is in the V-deconfinement phase, and holons and spinons start to hop coherently and independently as low-energy excitations. This indicates that the phenomenon of charge-spin separation[21] takes place and also the system is metallic.

Let us turn to the low-T region and see how the locations of these AF and MI phase transitions change. In Fig. 5, we present the specific heat C and C_{A_i} for $c_1 = 6.5$. We again found two peaks, at $c_4 \simeq 3.4$ and 5.4. Figures 5(b) and 5(c) show

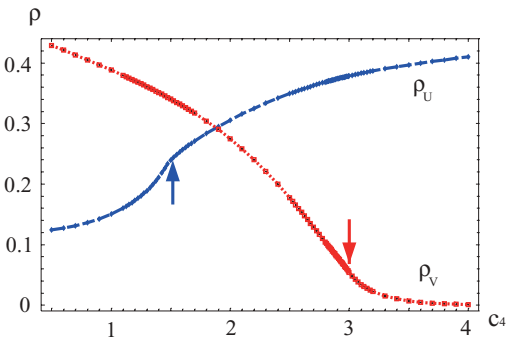

FIG. 4. (Color online) Instanton densities ρ_U and ρ_V as functions of c_4 for $c_1 = 3.5$, $c_5 = c_4/3.0$, and $L = 30$. Arrows indicate the phase transition points determined by the specific heat (see Fig. 2). At the first phase transition point, $c_4 \simeq 1.5$, ρ_U starts to increase. In contrast, at the second transition point, $c_4 \simeq 3.0$, ρ_V tends to vanish.

that both peaks develops systematically, indicating that both phase transitions are of second order. Individual specific heat in Fig. 5(d) shows that the peak of C at $c_4 \simeq 3.4$ corresponds to fluctuations of the c_4 and c_5 terms, and so the MI transition, while the peak at $c_4 \simeq 5.4$ is generated by the c_1 term and so the AF transition. Therefore the order of the AF and MI phase transitions along the c_4 axis has been interchanged compared to the previous high-T case of $c_1 = 3.5$.

To verify the preceding observation, we calculated the spin correlations, $G_s(r)$. The result is shown in Fig. 6. In the intermediate region $3.4 < c_4 < 5.4$, $G_s(r)$ exhibits very interesting behavior; that is, an AF correlation exists in a FM background. This implies coexistence of the FM and AF orders. We note that coexistence of FM and AM orders was also observed previously in the $CP^1 +$ Higgs boson model.[11,22] This model is a bosonic counterpart of the present model and the U(1) Higgs variable $\exp(i\alpha_x)$ there plays the role of the fermionic holon variable ψ_x.

In Fig. 7 we present instanton densities. Compared with the high-T result in Fig. 4, the result again indicates that two phase transitions have interchanged their order along the c_4 axis. As a result, there appears a range of c_4 in which both ρ_U and ρ_V are small, which implies that spinons and holons hop here in both U and V channels. In other words, charges are transported by holons, whereas spin degrees of freedom are transported by spinons in both the AF and the FM channels.

We repeated similar calculations for various values of c_1 and c_4 and obtained the phase diagram of the model for $c_5 = c_4/3.0$. In Fig. 8, we present the phase diagram: Fig. 8(a), in the c_4-c_1 plane and Fig. 8(b) in the δ-T plane, the latter is obtained from the former by using Eq. (2.35).

So far, we have studied the case of $c_5/c_4 = 1/3.0$. We also studied other values of the ratio c_5/c_4 and found a phase diagram similar to that in Fig. 8. As the value of c_5/c_4 is increased, the MI transition line shifts to the region of smaller δ. This is expected from Eq. (2.33) because a larger c_5/c_4 implies a smaller critical value of c_4 and, therefore, a smaller critical δ from Eq. (2.35).

To estimate roughly the critical δ of the MI transition, which we call $\delta_{\rm MI}$, for real materials, one may put $J \simeq 0.1$ eV, $t \simeq 0.3$ eV, so $J/t \simeq 1/3$. Then we have $\delta \sim (J/t)^2 \cdot (c_4/c_1) \simeq 0.1(c_4/c_1)$ from Eq. (2.35). For $c_1 \sim 10.0$ ($T \sim 100$ K), the critical line in Fig. 8(a) shows $c_4/c_1 \sim 0.4$, and this formula gives rise to $\delta_{\rm MI} \simeq 0.04$. As discussed following Eq. (2.33) the higher-order terms in Eq. (2.28) enhance the metallic phase, so the MI phase transition line is expected to be located in the very underdoped region $\delta \ll 1$.

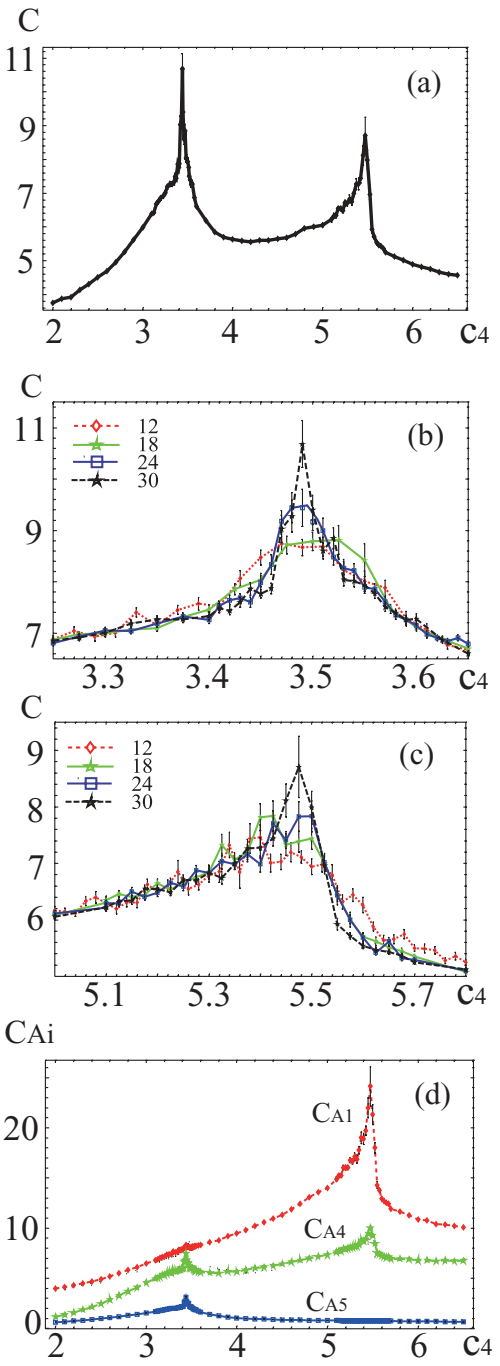

FIG. 5. (Color online) Specific heat C as a function of c_4 for $c_1 = 6.5$ and $c_5 = c_4/3.0$. (a) C for $L = 30$. There are two peaks, at $c_4 \simeq 3.4$ and 5.4. (b, c) Each peak of C develops as the system size is increased. Results indicate that both phase transitions are of second order. (d) Specific heat C_{A_i} of each term. Values indicate that the transition at $c_4 \simeq 3.4$ is the MI one and the transition at $c_4 \simeq 5.4$ is the AF one.

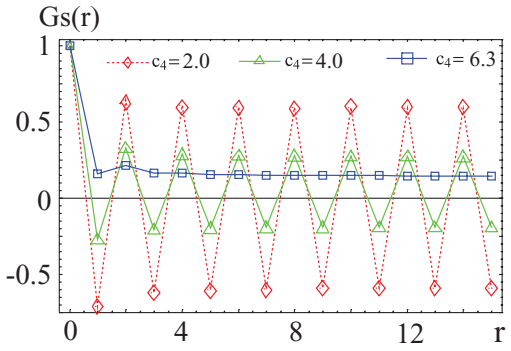

FIG. 6. (Color online) Spin correlation function $G_s(r)$ for $c_1 = 6.5$, $c_5 = c_4/3.0$, and $L = 30$. At $c_4 = 2.0$, the oscillatory behavior around 0 shows AF order. At $c_4 = 4.0$, there is AF order in the FM background order. At $c_4 = 6.3$, there is FM order.

IV. PHASE STRUCTURE OF THE FULL MODEL: SC TRANSITION

In this section, we study the full model of Eq. (2.40) with the action $A_{\rm full} = A_{\rm AF} + A_{\rm V} + A_{\rm M}$. Besides the AF and MI transitions observed in the previous section, we expect that the new term $A_{\rm M}$ in the action generates condensation of the hole-pair field $M_{x\mu}$ and/or the holon-pair field $M^{\star}_{x\mu}$ as the hole density δ is increased. This condensation implies the generation of an SC state.

We studied the system $A_{\rm full}$ by means of MC simulations. As $M^{\star}_{x\mu}$ is a composite of holons at x and $x+\mu$, we put $f_{1,2,3} \propto \delta^2 \propto c_4^2$ and $M^{\star}_{x\mu} \in U(1)$ as explained in Sec. II. Physically, the proportional constants f_i/c_4^2 $(i = 1,2,3)$ depend on the density of holes that actually participate in the SC fluid. We studied the system $A_{\rm full}$ for various values of f_i/c_4^2 and found that the system is stable only for the case with small values of f_i/c_4^2. For example, the AF phase disappears at a very small value of c_4 for $f_i/c_4^2 \sim O(1)$. In this section, we explicitly show the results for the case with $f_1 = f_2 = f_3 = 0.03\,c_4^2$.

Let us first study the high-T region first by choosing $c_1 = 4.0$, $c_5 = c_4/3.0$. In Fig. 9, we present various specific heats as

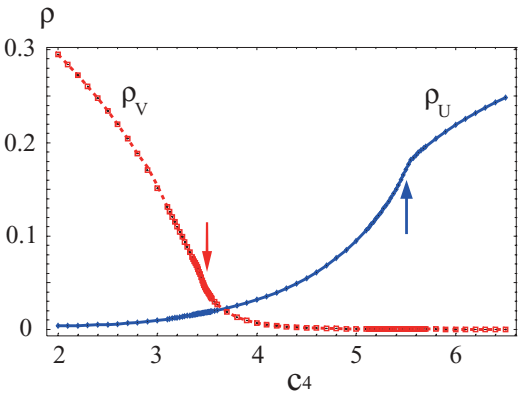

FIG. 7. (Color online) Instanton densities ρ_U and ρ_V as functions of c_4 for $c_1 = 6.5$, $c_5 = c_4/3.0$, and $L = 30$. Arrows indicate the phase transition points determined by the specific heat (see Fig. 5). At the first transition point $c_4 \simeq 3.4$, ρ_V tends to vanish. In contrast, at the second transition point $c_4 \simeq 5.4$, ρ_U gets large values, showing that the system enters the U-confinement phase.

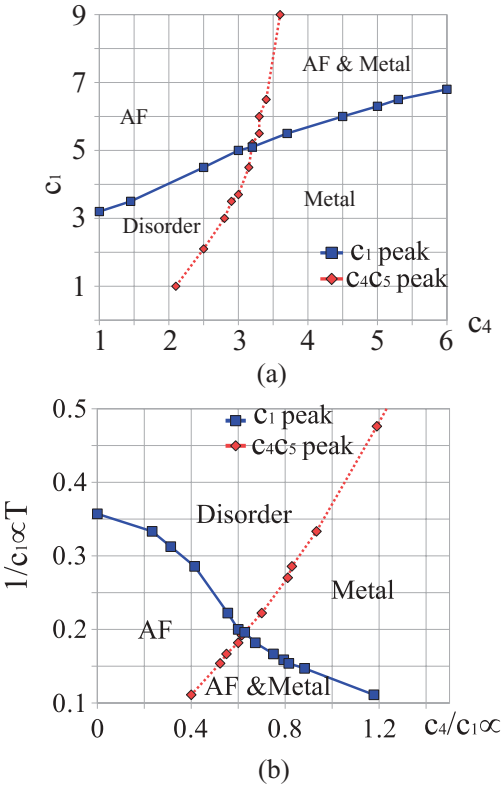

FIG. 8. (Color online) Phase diagram of the UV model for $c_5 = c_4/3.0$: (a) in the c_4-c_1 plane and (b) in the δ-T plane. Each phase is separated by two transition lines: the AF transition line and MI transition line. All transitions are of second order.

functions of c_4. The total specific heat C in Fig. 9(a) exhibits four peaks, at $c_4 \simeq 2.0$, 3.2, 3.5, and 4.1. To identify the physical meaning of each peak, we show the individual specific heat C_{A_i} in Fig. 9(b) and C_{f_i} $(i = 1,2,3)$ for the f_i term in A_M defined similarly to Eq. (3.2) in Fig. 9(c). From these results, it is expected that the first two peaks correspond to the AF transition at $c_4 \simeq 2.0$ and the MI transition at $c_4 \simeq 3.2$. The remaining two terms correspond to fluctuations of f terms in the action and, therefore, the SC phase transition. More precisely, the third peak, at $c_4 \simeq 3.5$, in C corresponds to the f_1, f_2 terms and the fourth one, at $c_4 \simeq 4.1$, to the f_1, f_3 terms. We comment on them later.

In Fig. 10 we present the spin correlation function $G_s(r)$ for various values of c_4. It is obvious that only at $c_4 = 1.2$ does AF LRO exist. At $c_4 = 5.0$, there is solid FM order. This is consistent with the preceding interpretation of the four peaks.

To study the symmetry of the SC state, we consider the quantity M_2, the expectation value of $M_{x\mu}\bar{M}_{x+\mu,\nu}$ $(\mu \neq \nu)$, defined as

$$M_2 \equiv \tfrac{1}{8}\langle M_{x+1,2}\bar{M}_{x1} + \bar{M}_{x+2,1}M_{x+1,2} + \bar{M}_{x2}M_{x+2,1} + \bar{M}_{x2}M_{x1}\rangle + \text{c.c.} \qquad (4.1)$$

In Fig. 11 we present M_2. It takes negative values and starts to develop significantly at $c_1 \sim 3.5$, that is, at the third peak of C. It is obvious that a d-wave correlation between adjacent hole-pair fields is generated beyond the third peak.

We also measured the instanton densities ρ_U, ρ_V, and $\rho_{M^\star}$. $\rho_{M^\star}$ is defined in a similar manner to ρ_U but by using the

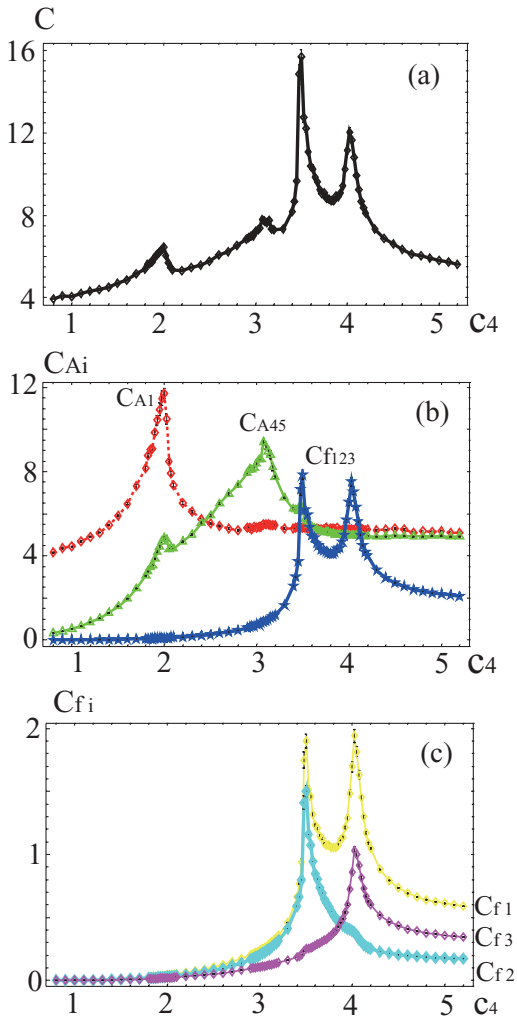

FIG. 9. (Color online) Specific heats (a) C, (b) C_{A_i}, and (c) C_{f_i} as functions of c_4 for $c_1 = 4.0$, $c_5 = c_4/3.0$, and $L = 24$. $C_{A_{45}}$ implies the fluctuation of $A_4 + A_5$; C_{f123}, that of $A_M = A_{f_1} + A_{f_2} + A_{f_3}$.

holon-pair field $M^{\star}_{x\mu}(\equiv M_{x\mu}U_{x\mu} \sim \bar{\psi}_{x+\mu}\bar{\psi}_x)$ instead of $U_{x\mu}$. $\rho_{M^{\star}}$ reflects the vortex density of $M^{\star}_{x\mu}$. These three instanton densities are shown in Fig. 12. By comparing Fig. 12 with Fig. 4 we see that the behavior of ρ_U and ρ_V is not influenced

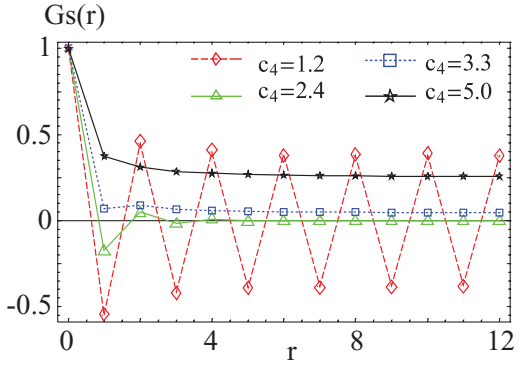

FIG. 10. (Color online) Spin correlation functions for various values of c_4 for $c_1 = 4.0$, $c_5 = c_4/3.0$, and $L = 24$. At $c_4 = 1.2$ there is AF order; at $c_4 = 2.4$, no magnetic order; at $c_4 = 3.3$, a tiny FM order; and at $c_4 = 5.0$, FM order.

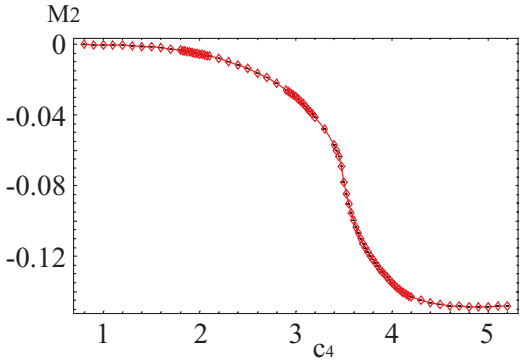

FIG. 11. (Color online) Expectation value M_2 of Eq. (4.1) for $c_1 = 4.0$, $c_5 = c_4/3.0$, and $L = 24$. The result shows that a d-wave correlation between adjacent hole-pair fields starts to appear at $c_4 \sim 3.5$.

strongly by the existence of the f terms; that is, ρ_U starts to increase at $c_4 \simeq 2.0$ and ρ_V vanishes at $c_4 \simeq 3.2$. The $M^{\star}$-instanton density $\rho_{M^{\star}}$ starts to decrease rapidly at $c_4 \simeq 3.5$ and vanishes at $c_4 \simeq 4.1$. We think that the SC phase transition, which is signaled by vanishingly small $\rho_{M^{\star}}$, takes place at $c_4 \simeq 4.1$.

From the preceding numerical calculations, we understand the physical meanings of the two peaks at $c_4 \simeq 3.5$ and 4.1 as follows. The third peak, at $c_4 \simeq 3.5$, is generated by the f_1 and f_2 terms and is located just after the MI transition at $c_4 \simeq 3.2$. After the MI transition, the holon-hopping amplitude $V_{x\mu}$ becomes stable, and as a result, these f_1 and f_2 terms start to correlate the phases of *a pair of adjacent link fields* $M^{\star}_{x\mu}$. In fact, these two terms in Eq. (2.43) need a stabilized $V_{x\mu}$ to let $M^{\star}_{x\mu}$ stabilize. Figure 12 shows that $\rho_{M^{\star}}$ at $c_4 \simeq 3.5$ is still large. So this effect is not strong enough to stabilize the holon-pair field $M^{\star}_{x\mu}$ completely in this region of c_4. To suppress vortex excitations of the holon-pair field $M^{\star}_{x\mu}$ (making $\rho_{M^{\star}}$ small enough), a sufficient amount of the f_3 term is necessary. The fourth peak of C, at $c_4 \simeq 4.1$, corresponds with the critical value of f_3 to realize such $M^{\star}_{x\mu}$ stabilization with phase coherence and generation of SC. These considerations lead to our conclusion that the genuine SC starts at the fourth peak, $c_4 \simeq 4.1$.

From the preceding consideration, we expect that the region between the third and the fourth peaks corresponds to a

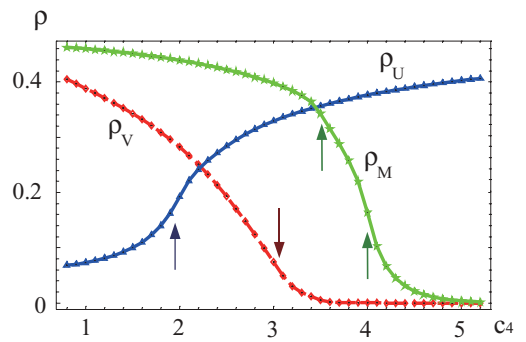

FIG. 12. (Color online) Instanton densities ρ_U, ρ_V, and $\rho_{M^{\star}}$ as a function of c_4 for $c_1 = 4.0$, $c_5 = c_4/3.0$, and $L = 12$. Arrows indicate the locations of the four peaks in C in Fig. 9.

primordial SC state. In this region we expect that holons acquire a pseudogap. In fact, as $M^{\star}_{x\mu}$ couples to ψ_x as $M^{\star}_{x\mu}\psi_{x+\mu}\psi_x$, a finite expectation value of $M^{\star}_{x\mu}$ supplies fermion-number-nonconserving hopping processes effectively. Together with the fermion-number-preserving hopping term supplied in $A_{\rm hop}$, these processes give rise to a gap in the excitation energy of holons.[23]

Furthermore, from the local gauge symmetry of the system, terms like $\bar{M}^{\star}_{x\mu}z_{x+\mu}z_x$ are also generated by the renormalization effect of high-energy modes of z_x and ψ_x. Then the spinon field z_x also acquires an extra contribution to its pseudogap, irrespective of a possible pseudogap expected by the mixing of two channels, $c_1U_{x\mu}z^{\star}_{x+\mu}z_x$ and $c_4V_{x\mu}\bar{z}_{x+\mu}z_x$. At any rate, the physical properties of that state, such as its excitation spectrum, are interesting and should be reserved as a future problem.

Next let us study the system $A_{\rm full}$ in the lower-T region by setting $c_1 = 6.5$, $c_5 = c_4/3.0$. Behaviors of various specific heats, C, C_{A_i}, and C_{f_i} are shown in Fig. 13. There are again four peaks in the total specific heat C: at $c_4 \simeq 3.4$, 3.6, 4.0, and 5.6. From the behavior of C_{A_i} and C_{f_i}, the first peak at, $c_4 \simeq 3.4$, corresponds to the MI transition; the peak(s) at $c_4 \simeq 4.0$ (and 3.6), to the SC transition; and the fourth peak, at $c_4 \simeq 5.6$, to the AF transition. The order of these transitions is different from that in the previous high-T case, as we have already seen in the UV model. To verify the preceding identification, we calculated $G_s(r)$, the expectation value of the adjacent hole-pair field M_2, and the instanton densities as before. We show the results in Figs. 14, 15, and 16. These results support the interpretation of each phase already given.

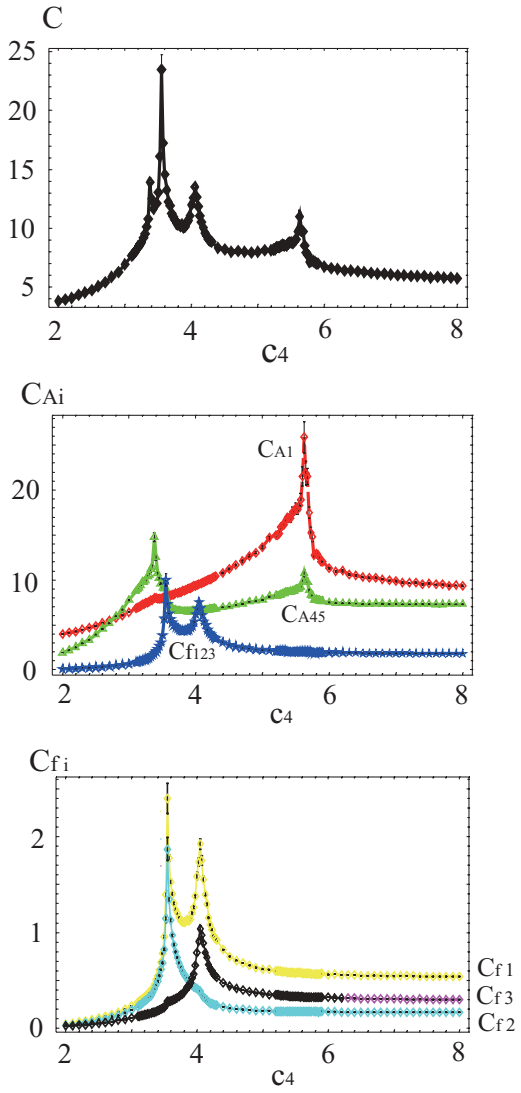

FIG. 13. (Color online) Specific heat C, C_{A_i}, and C_{f_i} as functions of c_4 for $c_1 = 6.5$, $c_5 = c_4/3.0$, and $L = 24$.

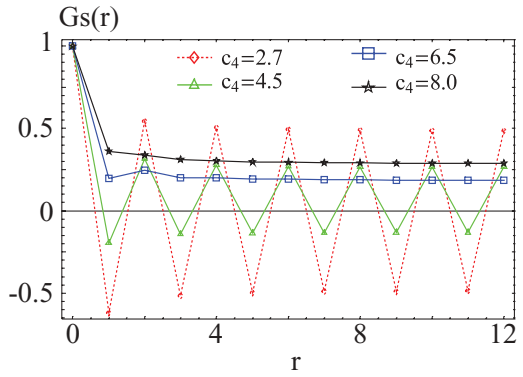

FIG. 14. (Color online) Spin correlation functions $G_s(r)$ for various values of c_4 with $c_1 = 6.5$ and $c_5 = c_4/3.0$. At $c_4 = 2.7$ there is AF order; at $c_4 = 4.5$, AF order in an FM background; and at $c_4 = 6.5$ and $c_4 = 8.0$, FM order.

In Fig. 17, we present the phase diagram obtained with the full model $Z_{\rm full}$ of Eq. (2.40) in the δ-T plane. Phases are separated by three transition lines, for AF, MI, and SC transitions. The SC phase always exists inside the metallic phase, whereas there is a phase of coexisting AF and SC in the low-T region. In addition to these three lines, one may add the line corresponding to the primordial SC transition as the line of pseudogap generation. Except for the pseudogap transition, which seems not to be a sharp transition in experiments, this phase diagram is consistent with that observed experimentally for homogeneous, clean, underdoped samples.[8]

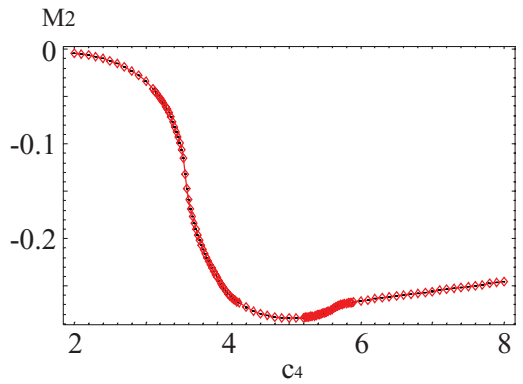

FIG. 15. (Color online) Expectation value M_2 for $c_1 = 6.5$, $c_5 = c_4/3.0$, and $L = 24$. The result shows that a d-wave correlation between adjacent hole-pair fields appears at $c_4 \sim 3.6$. It is interesting to observe that the correlation decreases slightly in the region *without* AF LRO $c_4 > 5.6$.

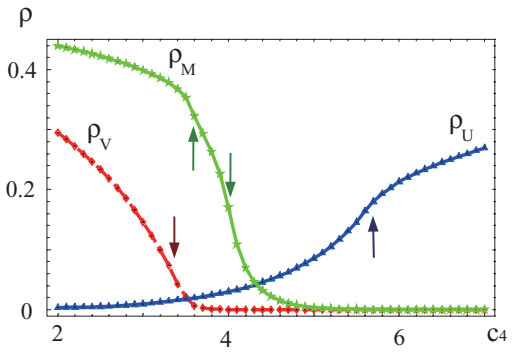

FIG. 16. (Color online) Instanton densities ρ_U, ρ_V, and ρ_M, as functions of c_4 for $c_1 = 6.5$, $c_5 = c_4/3.0$, and $L = 12$. Arrows indicate phase transition points determined by the specific heat (see Fig. 9). Their behavior is consistent with the phase transition discussed in the text based on Fig. 9.

V. CONCLUSION AND DISCUSSION

In the present paper, we have studied the phase structure in the underdoped region of the t-J model by using the slave-fermion representation. In this formalism, the AF-insulator phase naturally appears and it is expected that beyond a critical hole concentration $\delta_{\rm MI}$ the coherent hopping of holes is generated and the system enters into the metallic phase. This phenomenon was previously studied by the mean-field theory, and the critical hole concentration was estimated as $\delta_{\rm MI} = 0$.[24]

We have investigated the system by integrating out the fermionic holon field by the hopping expansion, which is legitimized for the region in and near the insulating phase, and then numerically studied the AF, MI and SC phase transitions. The obtained phase diagram is consistent with that observed experimentally for clean and homogeneous samples at low hole concentrations. The present study also implies that the

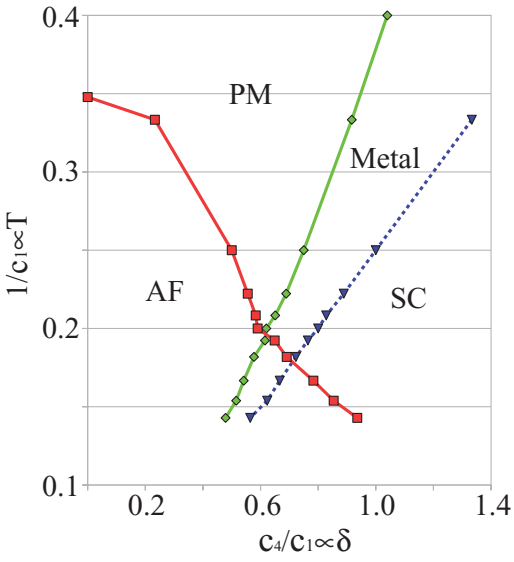

FIG. 17. (Color online) Phase diagram of the full model of Eq. (2.40) in the δ-T plane. The three lines, for the AF transition, MI transition, and SC transition, separate each phase. All transitions are of second order. One may add the pseudogap transition line as the fourth line.

observed pseudogap corresponds to a primordial formation of the SC order parameter $M_{x\mu}$.

For the SC phase transition, we have treated the coefficients of effective action in a more flexible manner than in the original hopping expansion, although we maintain the structure of interaction terms. As explained, this is because these coefficients certainly acquire renormalization and even change their signature as we go into the SC state. Some of the results in the present paper may reflect this flexibility; that is, they may not be possible in the original t-J model due to the restrictions among the coefficients. The pseudogap transition might disappear (merge to the genuine SC transition) with different treatments of the coefficients. Even in such a case, the results obtained in the present paper have important meaning as knowledge of a reference system for the t-J model and other canonical models of high-T_c materials.

Concerning the SC order parameter, we proposed the gauge-invariant $M_{x\mu}$ for hole pairs as the most direct possibility.[7] We have calculated its correlation function $\langle \bar{M}_{x\mu} M_{yv} \rangle$ but found no LRO of $M_{x\mu}$ even in the SC phase. We understand this in the following way. If one could calculate this correlation of the t-J model exactly, one would have LRO in the SC state. The effective model in exact treatment certainly contains a lot of nonlocal interaction terms among $M_{x\mu}$, although their coefficients are small. Nonvanishing LRO is to be supported by these nonlocal interactions. However, the present model truncates the effective interaction terms to short-range ones and, so, fails to produce LRO of $M_{x\mu}$.

However, the study of lattice gauge theory[25] provides us with a viable alternative for describing a SC state. An effective system may involve only short-range interactions but it may generate the Higgs phase, in which Meissner effects actually take place. The price to pay is that there are no local order parameters to signal LRO. Our present model, with the action A_M, is just such a model. Because our gauge-noninvariant $M^\star_{x\mu}$ for holon pairs has vanishing correlations owing to gauge-invariant action due to Elitzur's theorem,[26] one need to introduce complicated nonlocal order parameters[27] to show that some kind of LRO exists. Here we note that the existence of LRO is a beautiful theoretical criterion to demonstrate an SC phenomenon, but not a necessary condition. A simple and direct proof of an SC state may be to measure the mass of the external electromagnetic field and demonstrate the Meissner effect, that is, the Higgs mechanism. We have not made such a proof, but the existence of an anomalous peak of the specific heat certainly demonstrates a new phase, which should correspond to the Higgs phase. In fact, we have considered a U(1) Ginzburg-Landau model,[28] which is obtained from A_M of Eq. (2.43) by putting $V_{x\mu}$ to a certain constant. So the model loses gauge symmetry or can be viewed as a gauge-fixed version. The MC simulation of this model certainly exhibits a Higgs phase for sufficiently large f_i in which the correlation functions $\langle \bar{M}^\star_{x\mu} M^\star_{yv} \rangle$ exhibit LRO. Let us summarize the situation. Because the faithful effective model of $M_{x\mu}$ is full of nonlocal interactions, we replace it with a short-range model. By sacrificing the LRO of the gauge-invariant *local* order parameter, we are able to obtain the new phase. The analysis of the related model and the experience of lattice gauge theory strongly indicate that this phase is a Higgs phase that is necessary to support SC.

The reason we integrate out the fermionic holon field analytically is obvious; that is, it is technically difficult to study fermion systems by numerical methods. In recent years, however, it has become possible to numerically simulate relativistic fermion systems, and therefore it is important and also interesting to study the MI phase transition in the present system by means of those simulation methods. This problem is under study and we hope that the result will be reported in a future publication. Even in this situation, the content of the present paper may be useful as some basis and a reference for obtaining further understanding of physics of high-T_c superconductors.

Finally, it seems useful to compare the results obtained in this paper for the t-J model and the present knowledge of the 2D repulsive Hubbard model. In the intensive investigations for more than two decades, some aspects of the phase structure of the Hubbard model have been revealed. For example, the Néel state with AF long order appears to be the ground state at half-filling. For the doped case, many basic issues remain unknown, partly because numerical studies of a large system size have proven very difficult. However, very recently, an investigation using a constrained-path MC method has revealed some interesting aspects of the Hubbard model.[29] Upon doping at intermediate interaction strengths, the AF ordered state changes to a state with an incommensurate spin density wave (SDW) with long-wave modulation. In the SDW state, holes are delocalized and metallic behaviors appear. As the concentration of holes is increased beyond a critical value, the SDW order vanishes. As the strength of the interaction is increased there, some correlation develops in the charge sector, and it is expected that the system eventually evolves into a stripelike state. Therefore, these results for the Hubbard model shows some resemblance to the t-J model that we studied in this paper, though the stripelike state in the Hubbard model is to be replaced with the SC state in the t-J model.

ACKNOWLEDGMENTS

This work was partially supported by Grant-in-Aid for Scientific Research No. 20540264 from the Japan Society for the Promotion of Science.

APPENDIX A: EFFECT OF THERMAL MODES WITH NONVANISHING MATSUBARA FREQUENCIES

In this Appendix we discuss the effect of bosonic modes having nonvanishing Matsubara frequencies that we have ignored in the text. As a model, we consider a 3D lattice system of a complex boson field ϕ_x with the normal-ordered Hamiltonian $H_B(\phi)$, because our argument below is rather general and not restricted to the spinon field.

The partition function Z_ϕ for $H_B(\phi)$ is given by the path integral:[30]

$$Z_\phi = \int [d\phi] \exp\left[\int_0^\beta d\tau A_\phi(\tau)\right],$$
$$A_\phi(\tau) = -\sum_x \bar{\phi}_x(\tau)\partial_\tau \phi_x(\tau) - H_B[\phi(\tau)]. \tag{A1}$$

The boson field $\phi_x(\tau)$ is a function of the imaginary time $\tau \in [0,\beta]$. $\phi_x(\tau)$ satisfies the periodic boundary condition $\phi_x(0) = \phi_x(\beta)$ and is decomposed into Fourier series as

$$\phi_x(\tau) = \sum_{n=-\infty}^{\infty} \phi_{x,n} e^{i\omega_n \tau}, \quad \omega_n \equiv \frac{2\pi n}{\beta}, \tag{A2}$$

where ω_n is the Matsubara frequency. Then the first term of A_ϕ is expressed as

$$-\int_0^\beta d\tau \bar{\phi}_x(\tau)\partial_\tau \phi_x(\tau) = -\sum_n (2\pi n i)\bar{\phi}_{x,n}\phi_{x,n}. \tag{A3}$$

The H_B term of action A_ϕ is separated as

$$\int_0^\beta d\tau H_B[\phi_x(\tau)] = \beta H_B(\phi_0) + \beta H_1(\phi_0, \phi_{n\neq 0}) \tag{A4}$$

(we suppress the index x in $\phi_{x,n}$ if not necessary.) The first term, $H_B(\phi_0)$, contains only the zero modes ϕ_0, whereas the second term, $H_1(\phi_0,\phi_{n\neq 0})$, contains the interactions between the zero modes and the nonzero modes $\phi_{n\neq 0}$, and the self and spatial interactions among $\phi_{n\neq 0}$ themselves. Typical terms of $H_1(\phi_0,\phi_{n\neq 0})$ are given as

$$H_1 = \sum_x \Bigg[\sum_{n\neq 0} \bar{\phi}_{x,0}\phi_{x,0}\bar{\phi}_{x,n}\phi_{x,n} + \sum_{n,m\neq 0} (\bar{\phi}_{x,0}\bar{\phi}_{x,n}\phi_{x,m}\phi_{x,-n-m} + c.c.)\Bigg] + \cdots. \tag{A5}$$

Our treatment in the text corresponds to retaining only the zero modes ϕ_0 as the relevant variables at high T's and considering $\beta H_B(\phi_0)$ as their action. Of course, ϕ_0 are important because their condensation is necessary to form an ordered state with an off-diagonal LRO of ϕ_x. So the question is how the phase structure of the 3D system of ϕ_0 with action $\beta H_B(\phi_0)$ is to be modified by the effect of the remaining nonzero modes, $\phi_{n\neq 0}$.

One way to study it is to integrate out the nonzero modes in Eq. (A1) to obtain the effective action of ϕ_0 as

$$Z_\phi = \int [d\phi_0] e^{-\beta(H_B(\phi_{x,0}) + H_r(\phi_{x,0}))},$$
$$e^{-\beta H_r(\phi_{x,0})} \equiv \int [d\phi_{n\neq 0}] \exp\Bigg[-\sum_x \sum_{n\neq 0} (2\pi n i)\bar{\phi}_{x,n}\phi_{x,n} - \beta H_1(\phi_{x,0},\phi_{x,n\neq 0})\Bigg]. \tag{A6}$$

Although the behavior of the Green function of $\phi_{n\neq 0}$ depends on H_B, it is practical and general, to some extent, to assume the behavior

$$\langle \bar{\phi}_{x,n}\phi_{y,n}\rangle \sim \exp\left[-\sqrt{(2\pi n T/v)^2 + m_\phi^2 v^2}\,|x-y|\right] \tag{A7}$$

for $|x-y| \to \infty$. Here v is "the speed of light" of the bosonic excitation and m_ϕ is the energy gap. For example, for the spin-wave excitations above the ordered state, $v \propto Ja$ (a = lattice spacing) and $m_\phi = 0$. Equation (A7) corresponds to the case of excitations with a relativistic dispersion as in the Nèel state of antiferromagnets,[30] but similar exponential damping behavior appears for excitations having a nonrelativistic dispersion. Then the integration over $\phi_{n\neq 0}$ in Eq. (A6) using propagator

(A7) adds the renormalization term $H_r(\phi_0)$ in the effective action.

Without going into detail on the structure of $H_r(\phi_0)$, one can argue its effect based on physical grounds. First, for $m_\phi \neq 0$ the renormalization term $H_r(\phi_0)$ does not drastically change the phase structure of $H_B(\phi_0)$ because of the short-range nature of Eq. (A7). Concerning the qualitative effect of $H_r(\phi_0)$, it works in the direction of enhancing ordered states, that is, supporting the condensation of ϕ_0. This is because $\phi_{n\neq 0}$ become more relevant at lower T, as Eq. (A7) shows, and work to suppress the thermal fluctuations, which would potentially destroy the LRO. In short, the critical temperature for the ordered state should be raised by $H_r(\phi_0)$.

Next, let us consider the case of gapless excitations $m_\phi = 0$. As long as $T > 0$, the qualitative effect of $H_r(\phi_0)$ is the same as before, but somewhat enhanced as shown by Eq. (A7). At $T = 0$ a drastic change can be expected, because the Green functions, Eq. (A7), have only an algebraic decay, and therefore nonlocal interactions should be generated in $H_r(\phi_0)$ via integration over $\phi_{n\neq 0}$. Such nonlocal interactions may change the phase structure of the system and generate some new ordered states.[12]

In any case, the term $H_r(\phi_0)$ is more efficient at lower T, and it is physically expected that the renormalization enhances ordered states. Therefore, an ordered phase at finite T survives at lower T. This statement is actually supported by a couple of systems.[10,11]

APPENDIX B: HOLON-FIELD INTEGRATION

In this Appendix, we show some details of holon-field integration to derive Eq. (2.26). The same techniques are applicable for deriving $A_{\rm M}$ in Eq. (2.43). It is useful to start with the original path-integral expression,[7] in which the Grassmann number $\psi_x(\tau)$ is a function of the imaginary time τ. This is because the ordering of variables is crucial to obtain the correct results. Then the relevant integration reads as

$$\begin{aligned}
&\int d\psi_x d\psi_{x+\mu} \exp\left[\frac{c_3}{2\beta}\int_0^\beta d\tau\ (\bar{z}_{x+\mu}z_x)\bar{\psi}_x\psi_{x+\mu}(\tau) + \text{c.c.}\right] \\
&= \left(\frac{c_3}{2\beta}\right)^2 |\bar{z}_{x+\mu}z_x|^2 \\
&\quad\times \int_0^\beta d\tau_1 d\tau_2 \langle\bar{\psi}_{x+\mu}(\tau_1)\psi_x(\tau_1)\bar{\psi}_x(\tau_2)\psi_{x+\mu}(\tau_2)\rangle \\
&= -\left(\frac{c_3}{2\beta}\right)^2 |\bar{z}_{x+\mu}z_x|^2 \int_0^\beta d\tau_1 d\tau_2 \langle\psi_{x+\mu}(\tau_2)\bar{\psi}_{x+\mu}(\tau_1)\rangle \\
&\quad\times \langle\psi_x(\tau_1)\bar{\psi}_x(\tau_2)\rangle \\
&= \delta\left(\frac{c_3}{2}\right)^2 |\bar{z}_{x+\mu}z_x|^2, \qquad \text{(B1)}
\end{aligned}$$

where we have used the following Green function of the hopping expansion,

$$\langle\psi_x(\tau_1)\bar{\psi}_x(\tau_2)\rangle = \frac{e^{-m(\tau_1-\tau_2)}}{1+e^{-\beta m}}[\theta(\tau_1-\tau_2) - e^{-\beta m}\theta(\tau_2-\tau_1)]. \qquad \text{(B2)}$$

In Eq. (B2), m is the chemical potential and the following relation holds:

$$\delta = \langle\bar{\psi}_x(\tau+0)\psi_x(\tau)\rangle = \frac{e^{-\beta m}}{1+e^{-\beta m}}. \qquad \text{(B3)}$$

*Corresponding author: matsui@phys.kindai.ac.jp

[1] J. G. Bednorz and K. A. Müller, Z. Phys. B **64**, 189 (1986).

[2] See, e.g., N. Doiron-Leyraud, C. Proust, D. LeBoeuf, J. Levallois, J.-B. Bonnemaison, R. Liang, D. A. Bonn, W. N. Hardy, and L. Taillefer, Nature (London) **447**, 565 (2007); D. A. Bonn, Nature Phys. **2**, 159 (2006).

[3] For reviews of theoretical approaches, see, e.g., P. W. Anderson, *The Theory of Superconductivity in the High-Tc Cuprate Superconductors* (Princeton University Press, Princeton, NJ, 1997); P. A. Lee, N. Nagaosa, and X.-G. Wen, Rev. Mod. Phys. **78**, 17 (2006).

[4] P. W. Anderson, Science **235**, 1196 (1987).

[5] G. Kotliar and A. Ruckenstein, Phys. Rev. Lett. **57**, 1362 (1986), and references cited therein.

[6] G. Kotliar, Phys. Rev. B **37**, 3664 (1988); Y. Suzumura, Y. Hasegawa, and H. Fukuyama, J. Phys. Soc. Jpn. **57**, 2768 (1988).

[7] I. Ichinose and T. Matsui, Phys. Rev. B **45**, 9976 (1992); For the slave-boson approach, see **51**, 11860 (1995); I. Ichinose, T. Matsui, and M. Onoda, *ibid.* **64**, 104516 (2001).

[8] H. Mukuda, M. Abe, Y. Araki, Y. Kitaoka, K. Tokiwa, T. Watanabe, A. Iyo, H. Kito, and Y. Tanaka, Phys. Rev. Lett. **96**, 087001 (2006).

[9] The cuprates have a layer structure of 2D cupper-oxide planes in the xy plane stacked along the z axis. Reflecting it, the t-J model should have anisotropy in the coupling constants J and t in Hamiltonian (2.1) for the xy directions and z direction, that is, $J_z < J_{xy}$, $t_z < t_{xy}$. For explicit setup of asymmetry in the t-J model and calculation of the Neel temperature of the doped Heisenberg model, see H. Yamamoto, G. Tatara, I. Ichinose, and T. Matsui, Phys. Rev. B **44**, 7654 (1991). In this paper we report the formula for the symmetric case, for simplicity, except for the hole-pair action A_M in Eq. (2.43), but extension to the anisotropic case is straightforward.

[10] K. Sawamura, T. Hiramatsu, K. Ozaki, I. Ichinose, and T. Matsui, Phys. Rev. B **77**, 224404 (2008).

[11] K. Aoki, K. Sakakibara, I. Ichinose, and T. Matsui, Phys. Rev. B **80**, 144510 (2009).

[12] For the phase structure of nonlocal field theory, see G. Arakawa, I. Ichinose, T. Matsui, and K. Sakakibara, Phys. Rev. Lett. **94**, 211601 (2005); G. Arakawa, I. Ichinose, T. Matsui, K. Sakakibara, and S. Takashima, Nucl. Phys. B **732**, 401 (2006).

[13] The variable $z_x^\star$ should not be confused with $\bar{z}_x$ or z_x^*, the complex conjugate of z_x. In Ref. 7, the time-reversed spinon field $\tilde{z}_x \equiv i\sigma_2\bar{z}_x^{\rm t}, \tilde{z}_{x1} = \bar{z}_{x2}, \tilde{z}_{x2} = -\bar{z}_{x1}$ has been introduced. $z_x^\star$ here is just its complex conjugate, that is, $z_{x\sigma}^\star = \bar{\tilde{z}}_{x\sigma}$. In this paper an over bar implies the complex conjugate for a complex number and the Grassmann conjugate for a Grassmann number. We do not use asterisks here.

[14]We use the coefficient c_3 instead of c_2. This is partly because c_2 has been reserved for the coefficient of plaquette term $\bar{U}_{xv}\bar{U}_{x+v,\mu}U_{x+\mu,v}U_{x\mu}$, a possible interaction term that may be included in the generalization of the model. From this viewpoint, we set $c_2 = 0$ in this paper.

[15]Their explicit form and roles are discussed in detail in Ref. 7.

[16]F. A. Berezin, *The Method of Second Quantization* (Academic, New York, 1966); Y. Ohnuki and T. Kahsiwa, Prog. Theor. Phys. **60**, 548 (1978).

[17]We should remark that the signatures in front of λ_x and $\lambda_{x+\mu}$ in the exponent of $U_{x\mu}$ are the same, not the opposite. This is in contrast to the usual lattice gauge theory.

[18]S. Takashima, I. Ichinose, and T. Matsui, Phys. Rev. B **72**, 075112 (2005).

[19]Strictly speaking, $f_3 \propto \delta^4$ in the leading order. Here we take the simpler assumption, for simplicity of the numerical study.

[20]T. A. DeGrand and D. Toussaint, Phys. Rev. D **22**, 2478 (1980).

[21]P. W. Anderson, Phys. Rev. Lett. **64**, 1839 (1990); I. Ichinose and T. Matsui, Nucl. Phys. B **394**, 281 (1993); N. Nagaosa, Y. Inoue, T. Asanuma, and M. Imamura, Phys. Rev. Lett. **71**, 4120 (1993); I. Ichinose and T. Matsui, Phys. Rev. B **51**, 11860 (1995); I. Ichinose, T. Matsui, and M. Onoda, *ibid.* **64**, 104516 (2001).

[22]Y. Nakano, T. Ishima, N. Kobayashi, K. Sakakibara, I. Ichinose, and T. Matsui, e-print arXiv:1005.3997.

[23]The mechanism discussed here for generating a gap is a standard one through mixing of a normal channel and an SC channel. A typical example is the Bogoliubov transformation in the Bardeen-Cooper-Schriefer model of conventional SC. For bosonic spinon excitations, one needs a bosonic version of Bogoliubov transformation.

[24]B. I. Shraiman and E. D. Siggia, Phys. Rev. Lett. **61**, 467 (1988); Z. B. Su, Y. M. Li, W. Y. Lai, and L. Yu, *ibid.* **63**, 1318 (1989).

[25]J. Kogut, Rev. Mod. Phys. **51**, 655 (1979).

[26]S. Elitzur, Phys. Rev. D **12**, 3978 (1975).

[27]For the model including matter fields, the Wilson loop[25] exhibits the perimeter law even in the confinement phase, so it cannot be used as a nonlocal order parameter. For nonlocal order parameters in such a case, see, e.g., K. Fredenhagen and M. Marcu, Commun. Math. Phys. **92**, 81 (1983); K. Fredenhagen, M. Marcu, J. Bricmont, and J. Froehlich, Phys. Lett. B **122**, 73 (1983).

[28]T. Shimizu, S. Doi, I. Ichinose, and T. Matsui, Phys. Rev. B **79**, 092508 (2009); see also T. Ono, Y. Moribe, S. Takashima, I. Ichinose, T. Matsui, and K. Sakakibara, Nucl. Phys. B **764**, 168 (2007).

[29]C. C. Chang and S. Zhang, Phys. Rev. Lett. **104**, 116402 (2010), and references cited therein.

[30]See, e.g., the first citation in Ref. 7.